Cancer Immunol Immunother (2015) 64:1393–1406
DOI 10.1007/s00262-015-1743-z

ORIGINAL ARTICLE

Cytokine-enhanced maturation and migration to the lymph nodes of a human dying melanoma cell-loaded dendritic cell vaccine

Gabriela A. Pizzurro[1] · Ivana J. Tapia[1] · Leonardo Sganga[2] · Osvaldo L. Podhajcer[2] · José Mordoh[1,3,4] · María M. Barrio[1]

Received: 1 September 2014 / Accepted: 11 July 2015 / Published online: 22 July 2015

Abstract Dendritic cells (DCs) are professional APCs used for the development of cancer vaccines because of their ability to activate adaptive immune responses. Previously, we designed the DC/Apo-Nec vaccine using human DCs loaded with dying melanoma cells that primed Ag-specific cytotoxic T cells. Here, we evaluate the effect of a standard pro-inflammatory cytokine cocktail (CC) and adjuvants on DC/Apo-Nec maturation and migration. CC addition to the vaccine coculture allowed efficient Ag uptake while attaining strong vaccine maturation with an immunostimulatory profile. The use of CC not only increased CCR7 expression and the vaccine chemokine responsiveness but also upregulated matrix metalloproteinase-9 secretion, which regulated its invasive migration in vitro. Neither IL-6 nor prostaglandin E2 had a negative effect on vaccine preparation. In fact, all CC components were necessary for complete vaccine maturation. Subcutaneously injected DC/Apo-Nec vaccine migrated rapidly to draining LNs in nude mice, accumulating regionally after 48 h. The migrating cells of the CC-matured vaccine augmented in proportion and range of distribution, an effect that increased further with the topical administration of imiquimod cream. The migrating proportion of human DCs was detected in draining LNs for at least 9 days after injection. The addition of CC during DC/Apo-Nec preparation enhanced vaccine performance by improving maturation and response to LN signals and by conferring a motile and invasive vaccine phenotype both in vitro and in vivo. More importantly, the vaccine could be combined with different adjuvants. Therefore, this DC-based vaccine design shows great potential value for clinical translation.

Keywords Dendritic cell vaccine · Melanoma · Standard cytokine cocktail · Cell migration · Lymph node homing · Imiquimod cream

Abbreviations

Apo-Nec	Gamma-irradiated apoptotic–necrotic melanoma cells
CC	Standard pro-inflammatory cytokine cocktail
CFU	Colony-forming units
CM	Conditioned media
iDC	Immature dendritic cell
M26	HLA-A*0201-restricted MART-1-specific $CD8^+$ T cell
MMP	Matrix metalloproteinase
ON	Overnight
PGE2	Prostaglandin E2
rhuMMP-9	Recombinant human MMP-9

Electronic supplementary material The online version of this article (doi:10.1007/s00262-015-1743-z) contains supplementary material, which is available to authorized users.

✉ María M. Barrio
barrio.marcela@gmail.com

[1] Centro de Investigaciones Oncológicas – Fundación Cáncer (FUCA), Cramer 1180, CP 1426 Buenos Aires, Argentina

[2] Laboratorio de Terapia Molecular y Celular, Fundación Instituto Leloir - Instituto de Investigaciones Bioquímicas de Buenos Aires, Consejo Nacional de Investigaciones Científicas y Técnicas (CONICET), Buenos Aires, Argentina

[3] Laboratorio de Cancerología, Fundación Instituto Leloir - Instituto de Investigaciones Bioquímicas de Buenos Aires, Consejo Nacional de Investigaciones Científicas y Técnicas (CONICET), Buenos Aires, Argentina

[4] Instituto Alexander Fleming, Buenos Aires, Argentina

Introduction

DCs can initiate and direct adaptive immune responses due to their ability to stimulate naïve lymphocytes in an Ag-specific manner [1]. Many cancer immunotherapies have targeted DCs, directly or indirectly, for the induction of anti-tumour immune responses. Ex vivo-generated DC-based cancer vaccines are designed as adjuvant therapy to delay or prevent patient relapse through the induction of tumour-specific immunity to control microscopic, disseminated disease. Over the last 20 years, great progress has been made in understanding DC orchestration of anti-tumour immunity. DC-based vaccines have been tested in over 1,000 cancer patients [2, 3], though objective clinical responses have not fulfilled expectations, recording no or only modest outcomes [4]. However, these studies demonstrate a strong DC-based vaccine safety profile and the expansion of circulating TAA-specific $CD4^+$ and $CD8^+$ cells [5]. Therefore, optimal conditions must be developed for generating clinical-grade DC-based vaccines [6].

Multiple aspects must be defined in cancer vaccine design: first, the DC Ag-loading strategy, which will ultimately be responsible for the selection of Ag-specific anti-tumour $CD8^+$ T cells. This should be accompanied by timely DC maturation, which can be triggered either by recognition of pathogen-associated molecular patterns, by exposure to danger-associated molecular patterns released by injured/dying cells or through pro-inflammatory mediators [7, 8]. Administration of adjuvants, such as the TLR-7 ligand imiquimod [9] or GM-CSF [10], can also accelerate, prolong or enhance the vaccine-elicited Ag-specific immune response. DCs then migrate from peripheral tissues to the draining LNs through the lymphatic route, mainly driven by the CCR7-CCL19/CCL21 axis [11, 12] in different stages, determining their final localisation within the LN structure [13, 14]. During steady-state and inflammation, DCs utilise amoeboid mobilisation [15] as well as matrix metalloproteinases (MMPs), mainly MMP-9 [16, 17], to reach the lymphatic vessels and LNs. Despite optimising vaccine preparation in vitro, only a very small fraction of injected DCs reaches the draining LNs in intradermally vaccinated patients [18, 19], with the majority remaining at the injection site. Thus, research is focused on improving DC maturation, increasing CCR7 expression, chemokine-driven migration and IL-12 production to elicit strong anti-tumour T cell polarisation [20]. Although DC interactions with lymphocytes in the LN have been extensively studied [21], the newly reported role of the vaccination site in anti-tumour responses has recently led to an in situ analysis [22–24].

We have previously developed the DC/Apo-Nec vaccine, consisting of human monocyte-derived DCs cocultured with a mixture of gamma-irradiated apoptotic–necrotic allogeneic melanoma cell lines (Apo-Nec) [25, 26]. Apo-Nec offers immature DCs (iDCs), a full repertoire of known and yet unknown TAAs, as the vaccine activated MART-1- and gp100-specific $CD8^+$ cytotoxic T lymphocyte clones [25, 27]. The therapeutic melanoma DC/Apo-Nec vaccine has proven to be clinically safe, resulting in prolonged disease-free survival of 77.8 % stage II/III cutaneous melanoma patients for more than 8 years [28] (personal communication from Dr. Mordoh). In the present study, we continue our preclinical investigations to improve the DC/Apo-Nec vaccine performance through the addition of pro-inflammatory cytokines and adjuvants to its formulation. Specifically, we analysed the effect on DC maturation, Apo-Nec phagocytosis and vaccine immunostimulatory profile, as well as the impact on the DC/Apo-Nec vaccine migration both in vitro and in vivo.

Materials and methods

Mice

Eight- to twelve-week-old NIH nude mice were obtained from the Universidad Nacional de La Plata Animal Facility and bred at the Fundación Instituto Leloir under pathogen-free conditions in accordance with the guidelines of the Institute's Animal Care and Use Committee.

In vitro generation of DCs

Human DCs were derived from healthy donors' buffy coats, after giving written informed consent, with the approval of the Institutional Review Board, at the Instituto Alexander Fleming. Monocytes obtained from PBMCs were cultured as previously described [26]. At day 5, iDCs were ready to use and, when indicated, iDCs were purified through MACS with anti-CD14 or anti-DC-SIGN MicroBeads (Miltenyi Biotec, Germany), according to the manufacturer's instructions.

Apo-Nec preparation

Apo-Nec were obtained from the MEL-XY3 cell line, established in our laboratory and grown as previously described [25]. MEL-XY3 cells received a lethal 70 Gy gamma radiation dose (Siemens Lineal Accelerator, Instituto Alexander Fleming, Argentina). Viability and apoptotic–necrotic status was assessed as previously described [26].

Vaccine preparation and DC maturation

Apo-Nec were thawed immediately before use and cocultured with iDCs in AIM-V™ medium at a 1:3 ratio and a

final density of 1×10^6 cell/ml in a CO_2 incubator. When indicated, cocultures were supplemented with the CC, comprising 20 ng/ml TNF-α, 10 ng/ml IL-1β, 50 ng/ml IL-6 (Peprotech, México) and 1 μg/ml PGE2 (Calbiochem, CA, USA) and/or 2×10^4 colony-forming units (CFU)/ml BCG (kindly provided by Instituto Malbrán, Argentina), 1 μg/ml imiquimod (Glenmark Pharmaceuticals Ltd., Argentina) or 50 ng/ml GM-CSF (Laboratorio Pablo Cassará, Argentina). Alternatively, CC alone, 2 μg/ml LPS (*E. coli* J5, Sigma-Aldrich, MO, USA) or 10 ng/ml IL-10 were added to iDC as controls. Maturation status was assessed after 48-h coculture by DC phenotyping. DC/Apo-Nec + CC refers to the CC-matured vaccine only, since the CC was washed out prior to functional assays. Adjuvants were washed for in vitro experiments as well.

DC phenotyping

Cell surface markers were determined by mAbs (fluorochrome, clone): CD14 (FITC, M5E2), CD11c (PE, B-ly6), CD80 (FITC, L307.4), CD86 (FITC, FUN-1), CD83 (FITC, HB15e), CD1a (FITC, HI149), HLA-A/B/C (FITC, G46-2.6), HLA-DR/DP/DQ (FITC, Tu39), CD40 (FITC, 5C3), CCR5 (FITC, 2D5) and CCR7 (PE, 150503) (BD Biosciences, CA, USA) and PD-L1 (AlexaFluor 488, 130021) (R&D Systems, MN, USA), with the corresponding isotype controls. Samples were analysed by flow cytometry (FACSCalibur, BD) with the CellQuest Pro software (Becton–Dickinson, CA, USA); 5×10^5 cells were labelled per test, and 20,000 events were acquired for data analysis.

Phagocytosis assay

Apo-Nec phagocytosis was determined using a double-labelling strategy with PKH67 dye (Sigma-Aldrich, MO, USA) and anti-CD86 (PE, FUN-1, BD Biosciences, CA, USA). DCs were cocultured with $PKH67^+$ Apo-Nec in a CO_2 incubator, immunolabelled and analysed by flow cytometry; 48-h cocultures were compared to the initial vaccine mixture. The double-labelled population represents percentage of phagocytosis. Dye leaking and inhibitory temperature (4 °C) incubation controls were also performed. Data were analysed with the FlowJo software.

Cross-presentation assay

Vaccine MART-1-presenting capacity was tested using the HLA-A*0201-restricted MART-1-specific $CD8^+$ T cell (M26) clone (kindly provided by Dr Cassian Yee), as previously described [27]. Briefly, HLA-A*0201 DCs, obtained from CD14 MACS-purified monocytes, were used to prepare vaccine cocultures as described before. After 48 h, the M26 clone was added to the cocultures (1:3 effector/target ratio) and incubated overnight (ON). Supernatants were collected, centrifuged and stored at −80 °C for IFN-γ testing by enzyme-linked immunosorbent assay [29].

ELISA

Vaccine coculture and cross-presentation assay supernatants were tested to determine IL-10/IL-12 and IFN-γ levels, respectively. Determinations were performed with BD OptEIA human IL-10, IL-12p70 and IFN-γ ELISA kits (BD Biosciences, CA, USA) in triplicate, according to the manufacturer's instructions. A standard curve was included in each assay to quantify the samples.

Micro-chemotaxis chamber in vitro migration

DC/Apo-Nec vaccine migration was assessed using an AP48 micro-chemotaxis chamber (Neuroprobe Inc., MD, USA), according to the manufacturer's instructions. Chemotactic response was evaluated through 5-μm-pore polycarbonate membranes (Neuroprobe, Inc., MD, USA) towards 10 ng/ml CCL3 or CCL19 (Peprotech, Mexico) in AIM-V™ medium. Spontaneous and positive migration controls were performed; 5×10^4 DCs were loaded and allowed to migrate for 90 min in a CO_2 incubator. Membranes were fixed and stained with Giemsa, and five random 400× fields were analysed under the microscope. All conditions were tested in triplicate for each assay.

MMP gelatin zymography

Protease activity in the conditioned media (CM) was detected by gelatin zymography, as previously described [30]. Briefly, samples were separated by SDS-PAGE, using a 10 % acrylamide gel containing 1 mg/ml of gelatin Sigma G2500 (Sigma-Aldrich, USA) under non-reducing conditions, at 150 V for 60 min. After SDS was removed, gels were incubated at 37 °C in reaction buffer (50 mM Tris–HCl, 0.15 M NaCl, 10 mM $CaCl_2$, pH 7.4) ON, stained for observation and analysed with ImageJ software. Active recombinant human MMP-9 (rhuMMP-9) standard protein (Calbiochem, CA, USA) and incubation with 25 mM EDTA were included as controls.

Matrigel-coated transwell in vitro migration

Vaccine invasion assays were performed in 24-well format transwell inserts fitted with 8-μm-pore-size PET membranes (Becton–Dickinson, NJ, USA), towards 350 μl of 100 ng/ml CCL3, CCL19 or AIM-V™ medium alone. The upper chambers were coated with 70 μg of matrigel (BD Biosciences, MA, USA) and loaded with 2×10^5 cells in 200 μl

a

Maturation of iDC	Increment of marker-expressing cells ($CI_{95\%}$)			Increment of MFI ($CI_{95\%}$)	
	CD80	CD86	CD83	HLA-I	HLA-II
DC+LPS	(284.7 ± 161.9)% ↑*	(52.5 ± 30.2)% ↑*	(317.7 ± 225.1)% ↑*	(33.7 ± 50.2)% ↑	(29.9 ± 39.0)% ↑
DC+CC	(412.3 ± 99.8)% ↑*	(88.6 ± 7.2)% ↑*	(684.3 ± 159.4)% ↑*	(18.7 ± 43.7)% ↑	(56.3 ± 57.9)% ↑*
DC/Apo-Nec	(102.9 ± 103.5)% ↑	(56.8 ± 14.5)% ↑*	(27.4 ± 44.8)% ↑	(17.7 ± 15.9)% ↓	(1.4 ± 32.7)% ↑

b

DC/Apo-Nec vaccine	Modulation of marker-expressing cells ($CI_{95\%}$)			Modulation of MFI ($CI_{95\%}$)	
	CD80	CD86	CD83	HLA-I	HLA-II
+ CC	(213.6 ± 49.5)% ↑***	(38.8 ± 3.0)% ↑***	(566.4 ± 109,9)% ↑ ***	(78.9 ± 30.5)% ↑***	(79.3 ± 53.7)% ↑***
+ BCG	(5.4 ± 57.9)%	(-3.9 ± 25.3)%	(-12.7 ± 59.2)%	(-10.0 ± 42.6)%	(-18.8 ± 32.6)%
+ Imiquimod	(4.2 ± 76.0)%	(-2.3 ± 23.5)%	(-26.7 ± 74.0)%	(-30.0 ± 29.7)%	(-47.8 ± 19.6)%
+ GM-CSF	(13.0 ± 78.6)%	(-11.2 ± 32.9)%	(-18.8 ± 82.5)%	(-21.9 ± 31.3)%	(-47.4 ± 26.2)%

c

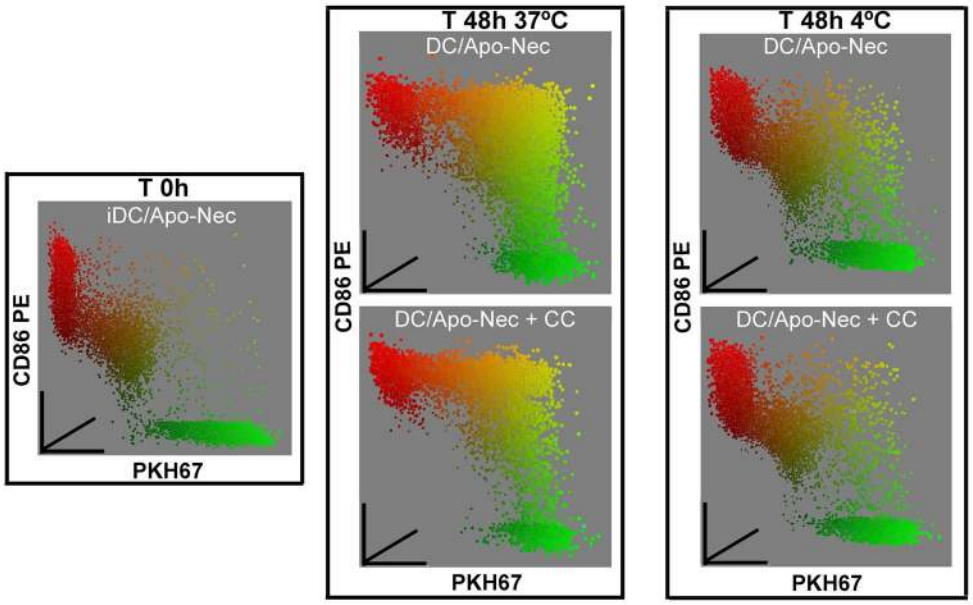

d

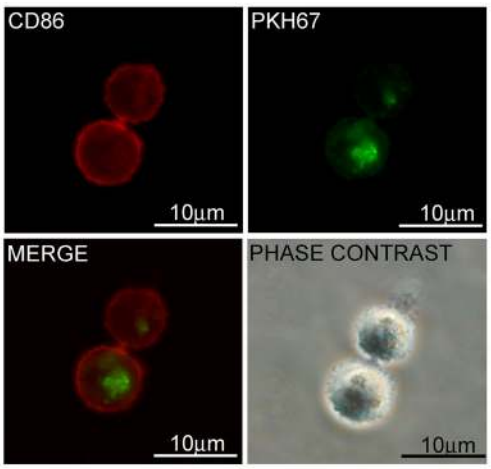

e

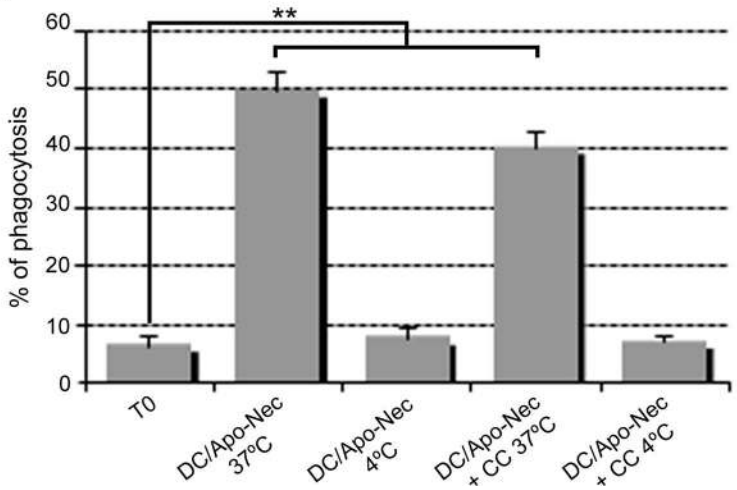

◀ **Fig. 1** DC/Apo-Nec vaccine maturation and Apo-Nec phagocytosis after 48-h coculture. **a** Modulation of costimulatory and Ag-presenting molecule expression in iDCs after exposure to different maturation stimuli (LPS, CC or Apo-Nec); $n = 8$. **b** Effect generated by the CC and adjuvant addition to the DC/Apo-Nec vaccine on cell surface maturation markers. Because no significant interaction was detected between treatments, only individual main effects are shown; $n = 3$. **c** Representative flow cytometric analysis of CD86 PE-labelled DCs cocultured with PKH67-stained Apo-Nec. Initial mixture of iDCs with Apo-Nec (T0 h) and 48-h cocultures (T48 h), along with corresponding 4 °C controls, are shown. Axis: x = PKH67, y = CD86 PE, z = forward scatter (FSC). **d** Double-stained vaccine coculture, showing $CD86^+$ DCs with traces of $PKH67^+$ Apo-Nec. Original magnification: 1000×. **e.** Percentage of phagocytosis after 48-h vaccine coculture. At 48 h, $CD86^+PKH67^+$ populations were compared to the initial vaccine mixture (T0 h) and the 4 °C incubation controls; $n = 6$. Results are expressed as 95 % confidence intervals ($CI_{95\ \%}$) of the percentage of effect size in tables and as Mean ± SEM in charts. $^*p < 0.05$, $^{**}p < 0.01$ and $^{***}p < 0.001$. DC/Apo-Nec + CC refers to the CC-matured vaccine

and incubated ON in a CO_2 incubator. Treatment with 1, 2 or 4 μM MMP-9 Inhibitor I (Calbiochem, CA, USA) and addition of 100, 200 or 300 ng/ml rhuMMP-9 were also included. Lower chamber media were analysed by flow cytometry and quantified by a fixed-time (60 s) acquisition.

In vivo vaccine LN homing

DC-SIGN MACS-purified iDCs were labelled with 1.75 μg/ml DiR (Molecular Probes, OR, USA) as previously described [31]. After 48 h, vaccine viability and maturation parameters were measured and 1.0×10^6 vaccine cells were inoculated in 50 μl PBS in the hindlimb footpad of nude mice. Isoflurane-anaesthetised mice were analysed using an IVIS Lumina Bioluminometer (Xenogen ex Caliper, Hopkinton, MA, USA); 48 h after injection, LNs were dissected and arranged in 96-well plates. LN nomenclature was taken from Van den Broeck et al. [32]. Images were analysed with the IVIS Living Image 3.0 software (Caliper Life Sciences). Migration was defined as DiR signal of the dissected ipsilateral LNs relative to the injection site, after background subtraction (contralateral LN). When indicated, a daily 12 μM MMP-9 Inhibitor I was administered locally. When used, 333 CFU of BCG were coinjected with the vaccine, or imiquimod 5 % cream (Imimore®, Laboratorio Panalab, Argentina) was topically administered on the injection site. Tumours were generated injecting 2.5×10^6 viable MEL-XY3 cells subcutaneously in the right lower flank 10 days prior to vaccine injection.

Detection of human DCs in mice LNs

DiR-labelled vaccines were injected in nude mice, and DiR^+ LNs were pooled and mechanically disaggregated. Contralateral LNs were used as a control. Cell suspensions were labelled with anti-human DC-SIGN FITC (Miltenyi Biotec,

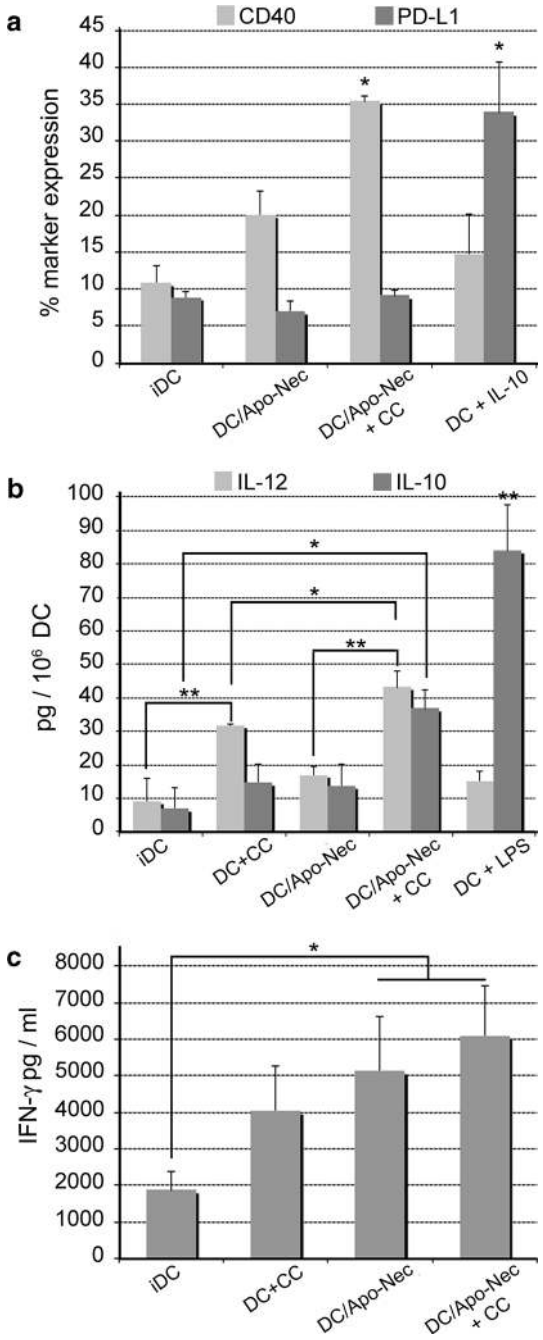

Fig. 2 Immunostimulatory profile of the DC/Apo-Nec vaccine. a The balance in immunomodulatory molecule expression was assessed by flow cytometry. After 48-h coculture, the expression of CD40 and PD-L1 in the vaccine was compared to iDCs. IL-10 was used to induce an immunosuppressive phenotype as a control; $n = 2$. **b** Supernatants were tested for both IL-12 and IL-10 by ELISA. Effect of CC addition to DC and vaccine cocultures was evaluated after 48 h. Maturation with LPS was used as control. Supernatants were tested in triplicate; $n = 3$. **c** After 48-h coculture, the vaccine was exposed in vitro to an Ag-specific T cell clone to determine its stimulatory capacity. Cells were cocultured ON with the MART-1-specific M26 clone, and IFN-γ release was assessed by ELISA; $n = 4$. Results are expressed as Mean ± SEM. $^*p < 0.05$ and $^{**}p < 0.01$. DC/Apo-Nec + CC refers to the CC-matured vaccine only, since the CC was washed out prior to functional assays

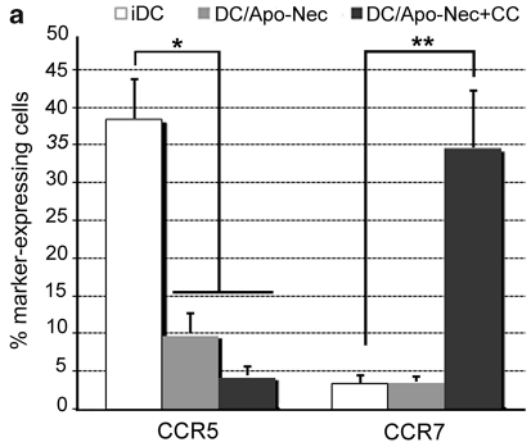

c

DC/Apo-Nec vaccine	Modulation of vaccine migration ($CI_{95\%}$)	
	CCL3	CCL19
+ CC	(10.1±25.8)% ↓	(39.9±15.3)% ↑ ***
+ BCG	(5.9±25.0)% ↑	(12.6±31.1)% ↑
+ Imiquimod	(4.4±42.8)% ↑	(4.5±7.3)% ↓
+ GM-CSF	(20.5±22.1)% ↓	(3.8±39.3)% ↑

Fig. 3 Vaccine CCR5/CCR7 expression and in vitro maturation-driven switch in the chemotactic response. **a** The balance in chemokine receptor CCR5 and CCR7 expression in DC. Expression in iDC and modulation after coculture with Apo-Nec was determined by flow cytometry; CCR5 $n = 8$ and CCR7 $n = 9$. **b** The change in iDC chemotactical response after exposure to different maturation stimuli was determined. Migration towards the CCR5-ligand CCL3 and the CCR7-ligand CCL19 was evaluated using a micro-chemotaxis chamber. The number of migrated cells was evaluated in triplicate; $n = 3$. **c** DC/Apo-Nec vaccine chemotaxis was evaluated after use of the CC and/or adjuvants BCG, imiquimod or GM-CSF. As no significant interaction was detected between treatments, only individual main effects are shown. The number of migrated cells was evaluated in triplicate; $n = 3$. Results are expressed as 95 % confidence intervals ($CI_{95\ \%}$) of the percentage of effect size in tables and as Mean ± SEM in charts. $^{*}p < 0.05$, $^{**}p < 0.01$ and $^{***}p < 0.001$. DC/Apo-Nec + CC refers to the CC-matured vaccine only, since the CC was washed out prior to functional assays. Adjuvants were washed for in vitro experiments as well

Germany) and anti-human CD11c PE before flow cytometric analysis. Furthermore, DC-SIGN MACS-purified DCs were labelled with 2 μg/ml Cell Tracker CM-DiI (Molecular Probes, Life Technologies), according to the manufacturer's instructions, to prepare vaccine cocultures for injection. At the indicated times, dissected LNs and injection sites were fixed in 4 % formaldehyde at 4ºC ON, cryopreserved in a 30 % w/v sucrose solution and placed on Optimal Cutting Temperature compound. Tissue sections were counterstained with Hoechst dye and mounted in Mowiol medium (Polysciences Inc., USA) for microscopic analysis.

Statistical analysis

All experiments were formulated with a randomised block design. Data from DCs obtained from each healthy donor were considered in blocks, for each assay. Data were analysed by two- or three-way ANOVA, depending on the experimental design. Main effect and multi-group analysis was performed by Tukey multiple comparisons. Statistical significance was considered with at least $\alpha = 0.05$ and indicated as $^{*}p < 0.05$, $^{**}p < 0.01$ and $^{***}p < 0.001$. Results are expressed as Mean ± SEM in charts and as 95 % confidence intervals ($CI_{95\ \%}$) of the percentage of effect size in tables. Sample sizes (n) correspond to the number of independent donor samples that were processed to generate DCs. The sample size and number of experimental replicates used for testing are both provided in figure captions. Data were analysed using InfoStat software (Universidad Nacional de Córdoba, Argentina).

Results

CC induces strong DC/Apo-Nec vaccine maturation while maintaining Ag-loading capacity

All iDCs were $CD11c^{+}$ and $CD14^{-}$ (data not shown), and after 48-h maturation with LPS or CC alone, we observed a considerable increase in CD80, CD86 and CD83 expression and slight modulation of the Ag-presenting molecules. Apo-Nec generated a mild effect on iDC maturation, with intermediate cell surface marker expression levels, mostly not significant compared with other maturation controls (Fig. 1a). Supplementing the DC/Apo-Nec vaccine with the CC strongly upregulated the expression of CD80, CD83, CD86, HLA-I and HLA-II (Fig. 1b). BCG, imiquimod and GM-CSF were tested alone and in combination with the CC during coculture, with no significant interaction between them. CC significantly increased up to five times the expression of the maturation markers of the DC/Apo-Nec vaccine ($p < 0.001$), while the Ag-presenting molecules HLA-I and HLA-II were increased by approximately 80 %. No additional effects were

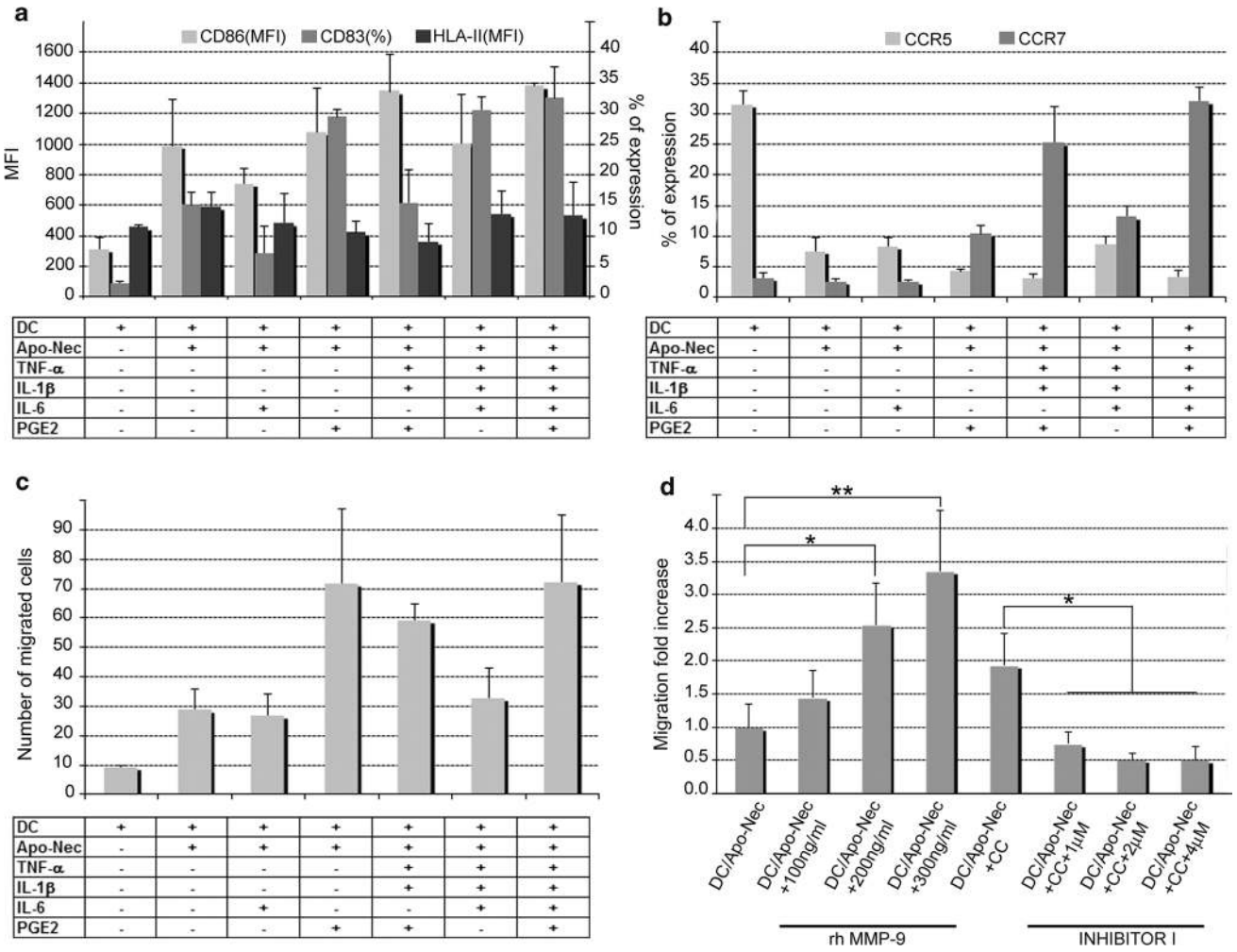

Fig. 4 Contribution of CC components in vaccine maturation and migration and the role of MMP-9 in vaccine invasive migration. The partial contribution of IL-6 and PGE2 on vaccine maturation and migration was evaluated after 48-h vaccine coculture. Cytokines either were added separately to the vaccine or were not included in the CC formulation, as indicated. **a** The effect on CD86, CD83 and HLA-II expression was analysed and compared to iDC, the vaccine alone or the use of the complete CC; $n = 2$. **b** The balance in CCR5 and CCR7 expression was analysed and compared to iDC, the vaccine alone or the use of the complete CC; $n = 2$. **c** The effect on the vaccine invasive migration in vitro was analysed. The number of migrated cells towards CCL19 was compared to iDC, the vaccine alone or the use of the complete CC; $n = 2$. **d** Vaccine invasive capacity towards CCL19 in vitro was mainly modulated by MMP-9 activity. Active recombinant human (rh)MMP-9 and MMP-9 Inhibitor I were added during vaccine coculture and migration assay. Fold increase in migrated cells relative to the DC/Apo-Nec vaccine is shown; $n = 4$. Results are expressed as Mean ± SEM. $^{*}p < 0.05$ and $^{**}p < 0.01$. DC/Apo-Nec + CC refers to the CC-matured vaccine only, since CC was washed out prior to functional assays

detected on DC/Apo-Nec maturation through the use of adjuvants during vaccine coculture (Fig. 1b, Supplementary Fig. 1). The constant, low MFI expression of CD1a was not significantly modulated in either case (Supplementary Fig. 1).

Apo-Nec proved to be a suitable multi-antigenic source for DC loading when formulating a more mature vaccine. The iDC and Apo-Nec populations could be clearly differentiated from one another immediately after vaccine preparation (Fig. 1c). After 48-h coculture at 37 °C, 50 % of the vaccine population was $CD86^{+}PKH67^{+}$, with DCs showing traces of Apo-Nec inside (Fig. 1c, d). Interestingly, despite inducing strong vaccine maturation, the addition of CC did not significantly impair iDC phagocytic capacity. Under these conditions, DC loading was slightly reduced compared with the DC/Apo-Nec vaccine, peaking at just over 40 % Ag capture by DCs (Fig. 1e). Phagocytosis was completely suppressed when cocultures were incubated at 4 °C (Fig. 1c, e).

CC modulates the immunostimulatory profile of the DC/Apo-Nec vaccine

To describe the DC/Apo-Nec vaccine immunological profile, we evaluated the paired expression of CD40/PD-L1 and the paired secretion of IL-12/IL-10 in vaccine CM along with the

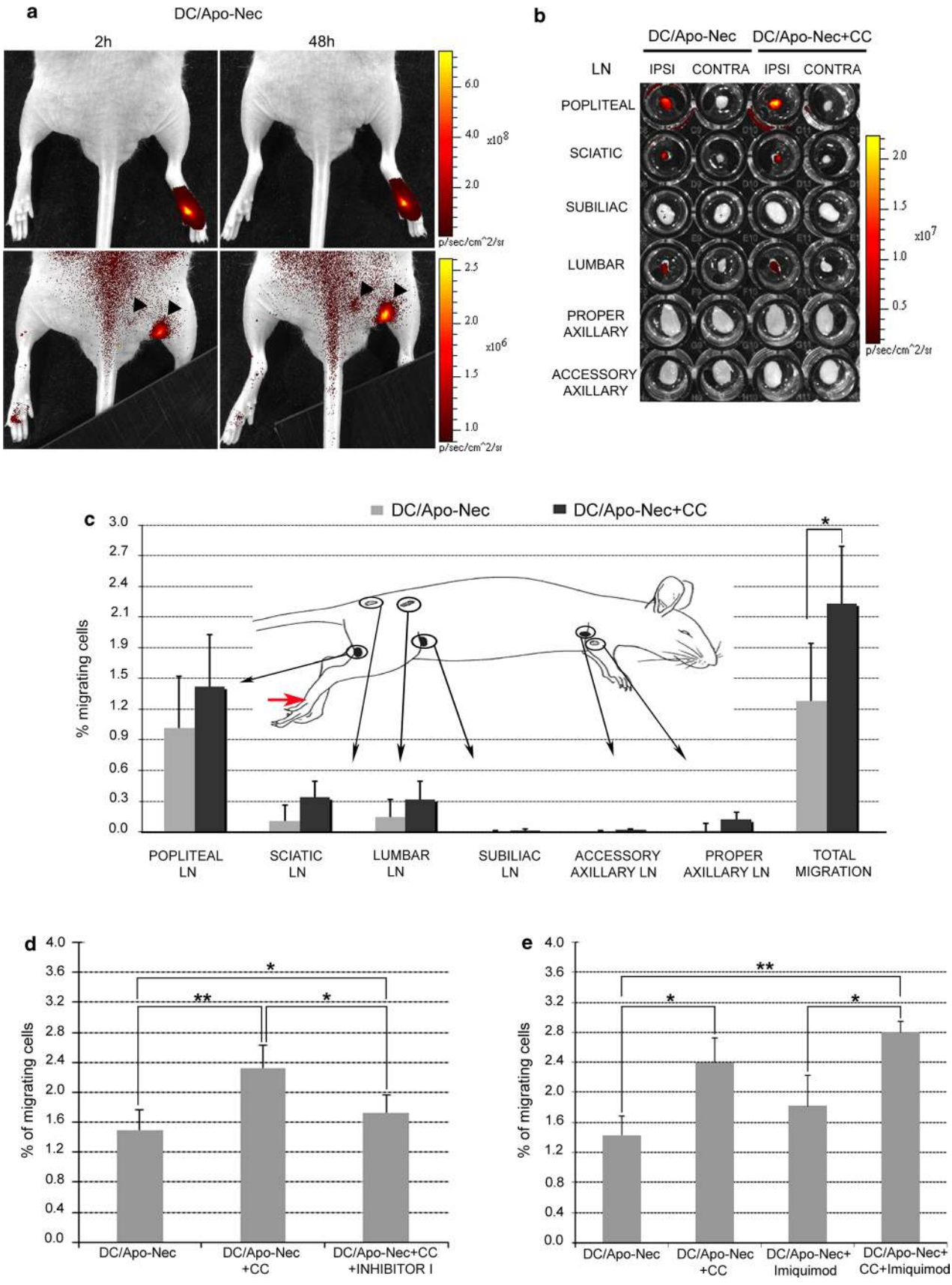
a
DC/Apo-Nec
2h
48h
6.0
4.0
x10^8
2.0
p/sec/cm^2/sr
2.5
2.0
x10^6
1.5
1.0
p/sec/cm^2/sr
b
DC/Apo-Nec
DC/Apo-Nec+CC
LN
IPSI
CONTRA
IPSI
CONTRA
POPLITEAL
SCIATIC
SUBILIAC
LUMBAR
PROPER AXILLARY
ACCESSORY AXILLARY
2.0
1.5
x10^7
1.0
0.5
p/sec/cm^2/sr
c
DC/Apo-Nec
DC/Apo-Nec+CC
% migrating cells
3.0
2.7
2.4
2.1
1.9
1.5
1.2
0.9
0.6
0.3
0.0
*
POPLITEAL LN
SCIATIC LN
LUMBAR LN
SUBILIAC LN
ACCESSORY AXILLARY LN
PROPER AXILLARY LN
TOTAL MIGRATION
d
% of migrating cells
4.0
3.6
3.2
2.8
2.4
2.0
1.6
1.2
0.8
0.4
0.0
*
**
*
DC/Apo-Nec
DC/Apo-Nec +CC
DC/Apo-Nec+CC +INHIBITOR I
e
% of migrating cells
4.0
3.6
3.2
2.8
2.4
2.0
1.6
1.2
0.8
0.4
0.0
**
*
*
DC/Apo-Nec
DC/Apo-Nec +CC
DC/Apo-Nec+ Imiquimod
DC/Apo-Nec+ CC+Imiquimod

◀ **Fig. 5** Vaccine migration in vivo and distribution to the LNs. **a** Representative images of a DC/Apo-Nec-injected mouse, at 2 and 48 h after inoculation. *Upper panels*: injection site in the hindlimb footpad. *Lower panels*: *black arrowheads* indicate the DiR^+ popliteal and sciatic LNs, visible after blocking the injection site. **b.** Representative image of the 96-well plate array of dissected LNs of injected mice at 48 h. Contralateral (CONTRA) to injection LN signal was considered as background of corresponding ipsilateral (IPSI) LNs. **c** Vaccine migration and distribution in the nude mice LNs after 48 h after injection. Total migration is composed of the sum of all the separate evaluated LNs. All percentages are referred to the fluorescence detected at the injection sites. The *red arrow* indicates the injection site; $n = 5$. **d** Vaccine migration performed in the presence of Inhibitor I in vivo. The drug was administered daily at the injection site of DC/Apo-Nec vaccine prepared with CC. It was compared to the migration of the vaccine alone after 48 h; $n = 3$. **e** Combination of the vaccine with the adjuvant imiquimod in vivo. Imiquimod cream was daily applied topically at the injection site for 48 h, when migration was analysed. Results are expressed as Mean ± SEM. $^*p < 0.05$ and $^{**}p < 0.01$. DC/Apo-Nec + CC refers to the CC-matured vaccine only, since CC was washed out prior to in vivo experiments

vaccine T cell-activating capacity. The costimulatory receptor CD40 was upregulated in DCs after coculture with Apo-Nec and significantly increased by CC addition ($p < 0.05$). This activation was associated with a constant, low expression of the T cell inhibitory ligand PD-L1, which could be induced by IL-10 (Fig. 2a). This pattern was observed when the vaccine was prepared combining the CC with different adjuvants (Supplementary Fig. 2a). Additionally, the slightly upregulated levels of Th1 cytokine IL-12 after coculture with Apo-Nec were significantly increased when CC was added, up to 150 % in the vaccine ($p < 0.01$), an effect that was not achieved with LPS (Fig. 2b). In addition, iDCs produced very low levels of the immunoregulatory cytokine IL-10, which were only slightly increased by the CC in the vaccine coculture, compared with the elevated levels induced by LPS (Fig. 2b). HLA-A*0201$^+$ DCs loaded with Apo-Nec strongly stimulated the MART-1-specific HLA-A*0201-restricted M26 clone, which significantly increased IFN-γ release ($p < 0.05$). T cell clone activation was similar in magnitude when induced by vaccine priming with an average twofold increase in basal iDC stimulation (Fig. 2c). Controls with MART-1 peptide-loaded DC and MART-1-expressing MEL-XY3 viable cells properly activated the M26 clone (data not shown).

CC improves Apo-Nec modulation of chemokine receptor expression and vaccine chemotaxis towards LN homing signals

To determine the vaccine sensitivity towards inflammatory or LN homing signals, the chemokine receptors CCR5 and CCR7 expression was assessed along with the in vitro response towards their ligands, CCL3 and CCL19, respectively. CCR5 was reduced by 75 % in iDCs after coculture with Apo-Nec, which in the presence of the CC decreased to 90 %. Conversely, the addition of the CC to the vaccine coculture was required to generate a significant increase in CCR7 expression, as Apo-Nec alone could not (Fig. 3a, Supplementary Fig. 2b). Neither adjuvant had an additional direct effect on the expression of either chemokine receptor (data not shown). Migration of DCs towards CCL3 was significantly impaired after exposure to different maturation stimuli, including coculture with Apo-Nec, with a corresponding increment in response to CCL19, despite expressing low CCR7 levels in the case of the DC/Apo-Nec vaccine (Fig. 3b). This response increased an additional 40 % with the use of the CC ($p < 0.001$), with no differences regarding CCL3. No changes in the chemotactic response of the vaccine were observed when BCG, imiquimod or GM-CSF were incorporated to the DC/Apo-Nec preparation (Fig. 3c).

CC-matured DC/Apo-Nec vaccine displays increased MMP-9 secretion and invasive migration

Vaccine CM contained the gelatinases MMP-9 and MMP-2, the former secreted by the DCs and the latter by Apo-Nec (Supplementary Fig. 3a). After 48-h incubation with LPS, CC or coculture with Apo-Nec, DCs significantly increased MMP-9 protease activity (Supplementary Fig. 3b, c). CC-induced vaccine maturation resulted in a 1.4-fold increase in MMP-9 secretion ($p < 0.001$), which was maintained in combination with the adjuvants that alone could not modify this parameter (Supplementary Fig. 3c, d). Vaccine migration through transwells reproduced the results observed in the chemotaxis chamber (data not shown). In matrigel-coated transwell assays, CC-matured DC/Apo-Nec vaccine exhibited an improved chemokine-driven motility. The limited response of the DC/Apo-Nec vaccine to CCL19 was enhanced almost 100 % by CC addition, along with a 75 % decrease in migration towards CCL3 ($p < 0.05$) compared with the 50 % reduction generated by the coculture of iDCs with Apo-Nec alone (Supplementary Fig. 3e).

Complete vaccine maturation requires all CC components, and the invasive migration depends on MMP-9 activity

We dissected the individual contribution of several CC components to vaccine maturation and migration in vitro, specifically IL-6 and PGE2, due to reported immunosuppressive functions [33, 34]. A combined increased expression of maturation markers, such as CD86, CD83 and HLA-II, was obtained with the use of the complete CC. However, PGE2 alone upregulated some of these parameters, while IL-6 alone could not, unless combined with other CC components (Fig. 4a). CCR7 expression was partially impaired when IL-6 was

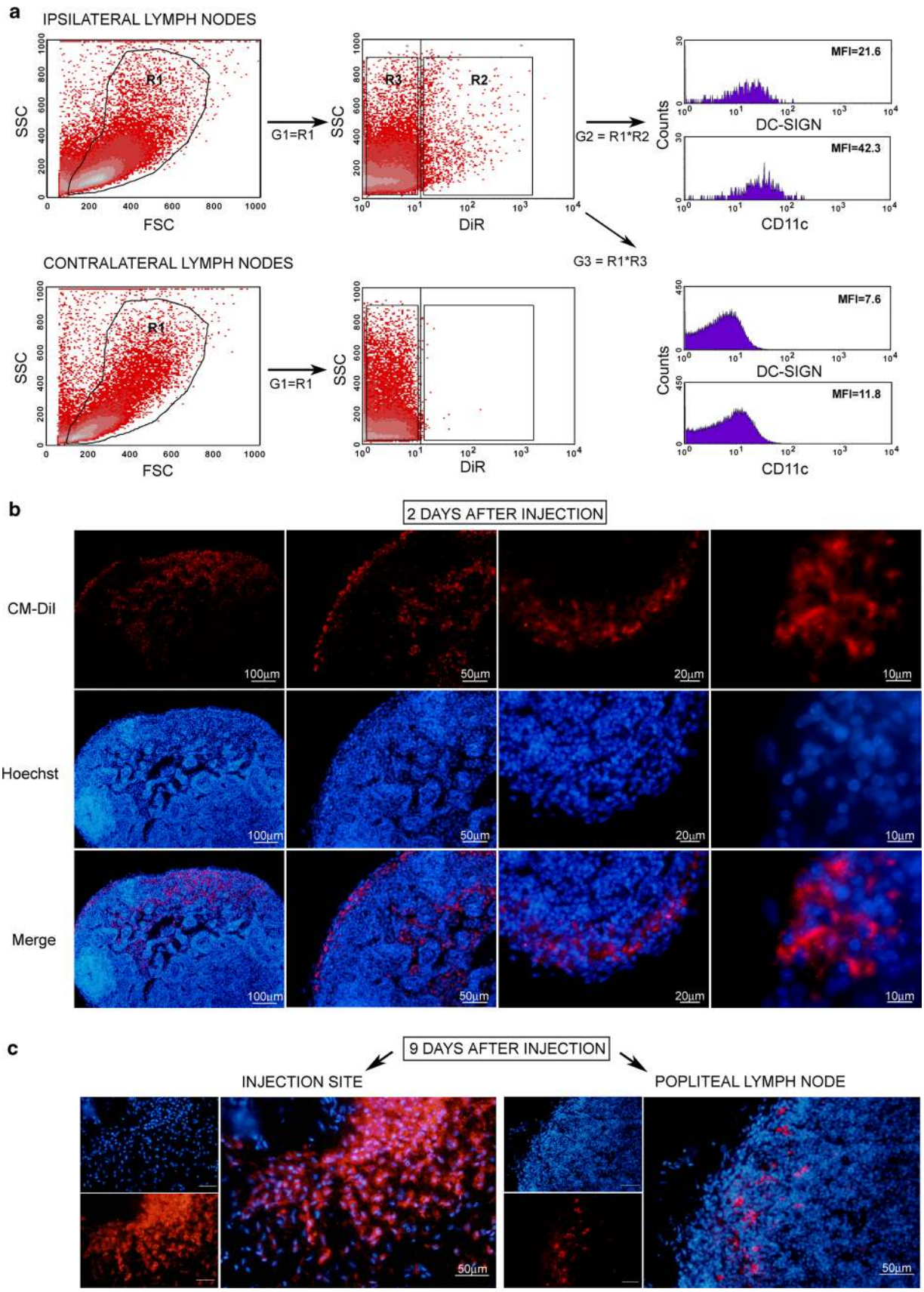
a
IPSILATERAL LYMPH NODES
SSC
FSC
R1
G1=R1
R3
R2
DiR
G2 = R1*R2
G3 = R1*R3
Counts
MFI=21.6
DC-SIGN
MFI=42.3
CD11c
CONTRALATERAL LYMPH NODES
MFI=7.6
MFI=11.8
b
2 DAYS AFTER INJECTION
CM-DiI
Hoechst
Merge
100μm
50μm
20μm
10μm
c
9 DAYS AFTER INJECTION
INJECTION SITE
POPLITEAL LYMPH NODE

◀**Fig. 6** Detection of human DCs in nude mouse LNs. **a** DiR^+ cells expressed human Ags DC-SIGN and CD11c in the LNs. After 48 h, DC/Apo-Nec vaccine-injected mouse LNs were dissected and disaggregated. Both ipsilateral and contralateral to injection LNs were analysed. After FSC/side-scatter gating on LN cells, DiR signal was determined. DiR^+ and DiR^- populations were analysed for human Ag expression. **b** Human DCs were localised within the LN structure after 48 h post-injection. After CM-DiI-labelled vaccine injection in mice, LNs were fixed and cryosectioned. Tissue sections were counterstained with Hoechst dye. Original magnification, from left to right: 100×, 200×, 400× and 1000×. **c** Vaccine homing to the LNs was detected for at least 9 days after injection. CM-DiI-labelled vaccines were injected in mice. After 9 days, both the skin injection site and the LNs were dissected. Samples were counterstained with Hoechst dye and analysed. Original magnification: 200×. DC/Apo-Nec + CC refers to the CC-matured vaccine only, since CC was washed out prior to in vivo experiments

present, though receptor expression reached its peak when using the complete CC (Fig. 4b). Vaccine invasive migration towards CCL19 was similarly improved by PGE2 alone and the complete CC (Fig. 4c). The augmented secretion of MMP-9, rather than an increase in CCR7, would be mainly responsible for the PGE2 effect (Fig. 4b, Supplementary Fig. 4a). To confirm the role of MMP-9 in vaccine invasive migration, we used the gelatinase-specific Inhibitor I and the rhuMMP-9 in the vaccine coculture for the transmigration assay. The CC-enhanced migration towards CCL19 was reversed when the MMP-9 inhibitor was added ($p < 0.05$), reaching similar levels to those obtained in the DC/Apo-Nec vaccine alone (Fig. 4d). The Inhibitor I affected only MMP-9 activity, as it did not change protease secretion to the vaccine CM (Supplementary Fig. 4b). Active rhuMMP-9 significantly augmented vaccine invasion, and its effect on DC/Apo-Nec was dose-dependent, attaining similar levels to that achieved by CC addition at 200 ng/ml ($p < 0.05$), which were further increased at the highest concentration tested ($p < 0.01$) (Fig. 4d).

CC-matured DC/Apo-Nec vaccine shows an increased imiquimod-modulated LN homing

DiR-labelled DC/Apo-Nec migration to the LNs was tracked through in vivo imaging after s.c. injection in nude mice. The vaccine was rapidly localised in the local ipsilateral draining LNs, evidenced 2 h after injection; 48 h after injection, the signal had accumulated in the regional popliteal and sciatic LNs, but the main DiR^+ fraction remained at the injection site (Fig. 5a) and the dissection of LNs confirmed that vaccine migration was ipsilateral to the injection site (Fig. 5b). A total of 1.3 ± 0.4 % of the DC/Apo-Nec vaccine migrated from the injection site, mostly to the popliteal LN, while CC-matured vaccine attained 2.2 ± 0.6 % ($p < 0.05$), with a wider distribution to the LNs. Though the primary migration went to the popliteal LN, a higher proportion of the CC-matured vaccine reached the sciatic and lumbar LNs and, strikingly, a low but very distinct signal was detected in the proper axillary LN (Fig. 5c). A reduction in the number of injected cells did not generate a change in the proportion of migrating vaccine (data not shown). Local administration of MMP-9 Inhibitor I at the injection site partially decreased CC-matured vaccine LN homing ($p < 0.05$) but was still significantly higher than the vaccine alone (Fig. 5d). Topical use of imiquimod cream at the injection site had an additive effect on CC-matured vaccine migration. Treatment with imiquimod alone was not sufficient for a major upregulation of this parameter after 48 h. However, the 20 % improvement of CC-matured vaccine migration represented a significant increase over basal migration ($p < 0.01$) (Fig. 5e). Local coadministration of BCG did not affect vaccine LN homing, neither did the presence of a regional tumour (Supplementary Fig. 5a, b).

The improved vaccine LN homing remains constant several days after injection

DiR^+ cells from ipsilateral LN disaggregates of injected mice expressed both human DC-SIGN and CD11c Ags, while contralateral LNs showed no DiR signal (Fig. 6a). After 48 h, CM-DiI-labelled DC/Apo-Nec cells were located within the mouse lymphoid structure, maintaining cellular integrity and homing mainly in the LN periphery but also penetrating into the LN structure (Fig. 6b). Long-term in vivo DiR monitoring of mouse LNs revealed an increasing proportion of CC-matured vaccine migration, reaching its maximum by the fifth day, which remained constant for at least 9 days after injection (Supplementary Fig. 5c). At this point, vaccine DC could be still localised not only in the LN cortical zone, but also in the skin injection site displaying normal morphology (Fig. 6c). The use of imiquimod cream did not affect the timeline of the CC-matured DC/Apo-Nec vaccine migration to the in vivo monitored regional LNs, but did change the distribution to the rest of the LNs analysed during the first 48 h, an effect that was reversed by the suspension of imiquimod treatment, evidenced 9 days after injection (Supplementary Fig. 5c, d).

Discussion

First, it is of great importance for DC/Apo-Nec vaccine preparation that the rapid acquisition of a robust mature phenotype through pro-inflammatory cytokines does not cause a significant impairment of Ag phagocytosis. Not only did DC capture Apo-Nec Ags, but also processed and properly loaded them for cross-presentation [35]. This

vaccine-generated T cell clone activation corroborates our earlier results [25] along with the strong allogeneic T cell stimulation observed with the CC-matured vaccine [26]. Thus, the use of the CC preserved the equilibrium required to generate Ag-specific immune responses [36], with a vaccine profile that would favour T cell stimulation and Th1 responses. The CC-matured vaccine was strongly sensitised for CD40L activation with low PD-L1 levels, dependent only on intrinsic basal levels. IL-12p70 secretion may seem quite modest [37], but higher levels reported using IFN-γ [38] or poly(I:C) [39], alone or combined with other stimuli, were associated with increased IL-10 release [40]. Adjuvants targeting DC TLRs, such as BCG or imiquimod, have been proven effective for DC maturation in vitro [41–43] but had no additional effect on the DC/Apo-Nec vaccine. The Apo-Nec may induce a maturation stimulus that overlies the TLR-ligand effect [7, 44] or may even suppress it, a situation that could be overcome with the complete CC. All the evaluated parameters were optimised with the complete CC, despite partial contributions or described immunosuppressive functions of some CC components [33, 34]. These facts highlight the delicate balance for DC optimal function, which must be carefully modulated in vitro to generate immunostimulatory DCs for therapeutic purposes.

Considering the improved CC-induced migrating phenotype in vitro, we performed a closer analysis of short- and mid-term human DC/Apo-Nec vaccine migration to the LNs in a more physiological environment, with the limitations of a xenogeneic model. Non-invasive in vivo cell-tracking techniques combined with near-infrared dyes are very powerful tools for cellular-based therapeutic research [45]. Even though the DC/Apo-Nec proportion that reached the LNs did not exceed previous results obtained with radiolabelled DCs in cancer patients [18, 19], in our studies this fraction could be underestimated due to partial cross-reaction between human and murine chemokines and adhesion molecules [11, 46]. MMP-9-driven DC migration through cytokine-induced maturation [17] was only partially responsible for DC/Apo-Nec vaccine LN homing, implying that other mechanisms are involved in this process, such as enhanced chemokine responsiveness. The less adhesive vaccine phenotype, which is also involved in the transit through interstitial compartments [16], may facilitate Ag encounter in conjunction with resident APCs at the injection site.

A more interesting result was the extensive distribution of the CC-matured DC/Apo-Nec vaccine to the LNs, further improved by the topical administration of imiquimod [9]. This tendency was maintained for at least a week, with vaccine DCs remaining both in the LNs and in the injection site. Although improving LN homing could still represent a challenge for DC-based vaccine development, there are no clear data regarding how many DCs are necessary to efficiently prime T cells or whether anti-tumour effective immune responses are only relevant in the LNs [47, 48]. Recent publications have suggested the vaccination site itself for Ag presentation, stimulating peripheral T lymphocytes with skin resident APCs in combination with adjuvants [23, 24]. Indeed, immunisation with a murine DC/Apo-Nec model has revealed the formation of tertiary lymphoid structures at the vaccination site [22]. This suggests that the therapeutic effect of the human DC/Apo-Nec vaccine [28] could emerge from the synergism of events taking place at the vaccination site in the dermis and in the draining LNs. Future experiments will focus on the evaluation of the in vivo immune response after DC/Apo-Nec vaccination in a humanised mouse model [49], which would help assess the vaccine capacity to elicit anti-tumour immunity [50], as well as the combination of adjuvants that could influence the fate and potency of those immune responses [9, 51].

To summarise, an effective DC-based vaccine should capture, process and load tumour Ags and then respond to specific chemokines to reach the draining LNs. In a pro-immunogenic LN environment, DCs could prime $CD4^+$ and $CD8^+$ naïve lymphocytes and trigger cellular and humoral immunity [52]. As DC may skew the immune response related to their maturation status and secreted cytokines, DC stimulating factors have been used to enhance their performance [37, 53]. In this study, we showed that the preparation of the clinically safe DC/Apo-Nec vaccine [28] with the "standard" maturation cocktail [8] induced inflammatory, Ag-loaded and T cell-activating DCs. After s.c. injection, the vaccine migrated to regional LNs, aided by the imiquimod adjuvant and demonstrated a rapid and long-lasting homing, which may allow multiple rounds of T lymphocyte screening with an improved anti-tumour immune response, yet to be tested in an appropriate in vivo model. These results constitute solid and promising preclinical evidence supporting the use of the CC-matured DC/Apo-Nec vaccine for melanoma treatment.

Acknowledgments This work was supported by Grants from CONICET, Agencia Nacional de Promoción Científica y Tecnológica (ANPCyT), Instituto Nacional del Cáncer—Ministerio de Salud de la Nación Argentina (INC-MSal), Fundación Sales, Fundación Cáncer, Fundación Pedro F. Mosoteguy and Fundación María Calderón de la Barca, Argentina. Drs José Mordoh, María M. Barrio and Osvaldo L. Podhajcer are members of CONICET, and Gabriela A. Pizzurro, Ivana J. Tapia and Leonardo Sganga are fellows of the same institution. We thank Adriana Fontanals, Sonia Mohr and Jimena Afonso for their technical assistance at the Fundación Instituto Leloir. We also thank the Servicio de Hemoterapia for the supply of blood samples and the Servicio de Anatomía Patológica for tissue sample processing and cryosectioning facilities, from the Instituto Alexander Fleming.

Compliance with ethical standards

Conflict of interest The authors declare that they have no commercial or financial conflict of interest.

Ethical standards Animal studies have been approved by the Animal Care and Use Committee from the Fundación Instituto Leloir. The use of healthy donor blood samples for DC isolation has been approved by the Comité de Ética en Investigación from the Instituto Alexander Fleming. The manuscript does not contain clinical studies or patient data.

References

1. Banchereau J, Steinman RM (1998) Dendritic cells and the control of immunity. Nature 392(6673):245–252
2. Ridgway D (2003) The first 1000 dendritic cell vaccinees. Cancer Invest 21(6):873–886
3. Vacchelli E, Vitale I, Eggermont A, Fridman WH, Fucikova J, Cremer I, Galon J, Tartour E, Zitvogel L, Kroemer G, Galluzzi L (2013) Trial watch: dendritic cell-based interventions for cancer therapy. Oncoimmunology 2(10):e25771. doi:10.4161/onci.25771
4. Palucka K, Ueno H, Roberts L, Fay J, Banchereau J (2010) Dendritic cells: are they clinically relevant? Cancer J 16(4):318–324
5. Madan RA, Gulley JL, Fojo T, Dahut WL (2010) Therapeutic cancer vaccines in prostate cancer: the paradox of improved survival without changes in time to progression. Oncologist 15(9):969–975
6. Pizzurro GA, Barrio MM (2015) Dendritic cell-based vaccine efficacy: aiming for hot spots. Front Immunol 6:91. doi:10.3389/fimmu.2015.00091
7. Escamilla-Tilch M, Filio-Rodriguez G, Garcia-Rocha R, Mancilla-Herrera I, Mitchison NA, Ruiz-Pacheco JA, Sanchez-Garcia FJ, Sandoval-Borrego D, Vazquez-Sanchez EA (2013) The interplay between pathogen-associated and danger-associated molecular patterns: an inflammatory code in cancer? Immunol Cell Biol 91(10):601–610
8. Jonuleit H, Kuhn U, Muller G, Steinbrink K, Paragnik L, Schmitt E, Knop J, Enk AH (1997) Pro-inflammatory cytokines and prostaglandins induce maturation of potent immunostimulatory dendritic cells under fetal calf serum-free conditions. Eur J Immunol 27(12):3135–3142
9. Fehres CM, Bruijns SC, van Beelen AJ, Kalay H, Ambrosini M, Hooijberg E, Unger WW, de Gruijl TD, van Kooyk Y (2014) Topical rather than intradermal application of the TLR7 ligand imiquimod leads to human dermal dendritic cell maturation and CD8 T-cell cross-priming. Eur J Immunol 44(8):2415–2424
10. Barrio MM, de Motta PT, Kaplan J, von Euw EM, Bravo AI, Chacon RD, Mordoh J (2006) A phase I study of an allogeneic cell vaccine (VACCIMEL) with GM-CSF in melanoma patients. J Immunother 29(4):444–454
11. Campbell JJ, Bowman EP, Murphy K, Youngman KR, Siani MA, Thompson DA, Wu L, Zlotnik A, Butcher EC (1998) 6-C-kine (SLC), a lymphocyte adhesion-triggering chemokine expressed by high endothelium, is an agonist for the MIP-3beta receptor CCR7. J Cell Biol 141(4):1053–1059
12. Johnson LA, Jackson DG (2014) Control of dendritic cell trafficking in lymphatics by chemokines. Angiogenesis 17(2):335–345
13. MartIn-Fontecha A, Sebastiani S, Hopken UE, Uguccioni M, Lipp M, Lanzavecchia A, Sallusto F (2003) Regulation of dendritic cell migration to the draining lymph node: impact on T lymphocyte traffic and priming. J Exp Med 198(4):615–621
14. Alvarez D, Vollmann EH, von Andrian UH (2008) Mechanisms and consequences of dendritic cell migration. Immunity 29(3):325–342
15. Renkawitz J, Schumann K, Weber M, Lammermann T, Pflicke H, Piel M, Polleux J, Spatz JP, Sixt M (2009) Adaptive force transmission in amoeboid cell migration. Nat Cell Biol 11(12):1438–1443
16. Ratzinger G, Stoitzner P, Ebner S, Lutz MB, Layton GT, Rainer C, Senior RM, Shipley JM, Fritsch P, Schuler G, Romani N (2002) Matrix metalloproteinases 9 and 2 are necessary for the migration of Langerhans cells and dermal dendritic cells from human and murine skin. J Immunol 168(9):4361–4371
17. Yen JH, Khayrullina T, Ganea D (2008) PGE2-induced metalloproteinase-9 is essential for dendritic cell migration. Blood 111(1):260–270
18. Ridolfi R, Riccobon A, Galassi R, Giorgetti G, Petrini M, Fiammenghi L, Stefanelli M, Ridolfi L, Moretti A, Migliori G, Fiorentini G (2004) Evaluation of in vivo labelled dendritic cell migration in cancer patients. J Transl Med 2(1):27. doi:10.1186/1479-5876-2-27
19. De Vries IJ, Krooshoop DJ, Scharenborg NM, Lesterhuis WJ, Diepstra JH, Van Muijen GN, Strijk SP, Ruers TJ, Boerman OC, Oyen WJ, Adema GJ, Punt CJ, Figdor CG (2003) Effective migration of antigen-pulsed dendritic cells to lymph nodes in melanoma patients is determined by their maturation state. Cancer Res 63(1):12–17
20. Vicari AP, Vanbervliet B, Massacrier C, Chiodoni C, Vaure C, Ait-Yahia S, Dercamp C, Matsos F, Reynard O, Taverne C, Merle P, Colombo MP, O'Garra A, Trinchieri G, Caux C (2004) In vivo manipulation of dendritic cell migration and activation to elicit antitumour immunity. Novartis Found Symp 256:241–254
21. Henrickson SE, Perro M, Loughhead SM, Senman B, Stutte S, Quigley M, Alexe G, Iannacone M, Flynn MP, Omid S, Jesneck JL, Imam S, Mempel TR, Mazo IB, Haining WN, von Andrian UH (2013) Antigen availability determines CD8(+) T cell-dendritic cell interaction kinetics and memory fate decisions. Immunity 39(3):496–507
22. Mac Keon S, Gazzaniga S, Mallerman J, Bravo AI, Mordoh J, Wainstok R (2010) Vaccination with dendritic cells charged with apoptotic/necrotic B16 melanoma induces the formation of subcutaneous lymphoid tissue. Vaccine 28(51):8162–8168
23. Harris RC, Chianese-Bullock KA, Petroni GR, Schaefer JT, Brill LB 2nd, Molhoek KR, Deacon DH, Patterson JW, Slingluff CL Jr (2012) The vaccine-site microenvironment induced by injection of incomplete Freund's adjuvant, with or without melanoma peptides. J Immunother 35(1):78–88
24. Hailemichael Y, Dai Z, Jaffarzad N, Ye Y, Medina MA, Huang XF, Dorta-Estremera SM, Greeley NR, Nitti G, Peng W, Liu C, Lou Y, Wang Z, Ma W, Rabinovich B, Sowell RT, Schluns KS, Davis RE, Hwu P, Overwijk WW (2013) Persistent antigen at vaccination sites induces tumor-specific CD8(+) T cell sequestration, dysfunction and deletion. Nat Med 19(4):465–472
25. von Euw EM, Barrio MM, Furman D, Bianchini M, Levy EM, Yee C, Li Y, Wainstok R, Mordoh J (2007) Monocyte-derived dendritic cells loaded with a mixture of apoptotic/necrotic melanoma cells efficiently cross-present gp100 and MART-1 antigens to specific CD8(+) T lymphocytes. J Transl Med 5:19. doi:10.1186/1479-5876-5-19
26. Pizzurro GA, Madorsky Rowdo FP, Pujol-Lereis LM, Quesada-Allue LA, Copati AM, Roberti MP, Teillaud JL, Levy EM, Barrio MM, Mordoh J (2013) High lipid content of irradiated human melanoma cells does not affect cytokine-matured dendritic cell function. Cancer Immunol Immunother 62(1):3–15
27. Barrio MM, Abes R, Colombo M, Pizzurro G, Boix C, Roberti MP, Gelize E, Rodriguez-Zubieta M, Mordoh J, Teillaud JL (2012) Human macrophages and dendritic cells can equally present MART-1 antigen to CD8(+) T cells after phagocytosis

of gamma-irradiated melanoma cells. PLoS One 7(7):e40311. doi:10.1371/journal.pone.0040311
28. von Euw EM, Barrio MM, Furman D, Levy EM, Bianchini M, Peguillet I, Lantz O, Vellice A, Kohan A, Chacon M, Yee C, Wainstok R, Mordoh J (2008) A phase I clinical study of vaccination of melanoma patients with dendritic cells loaded with allogeneic apoptotic/necrotic melanoma cells. Analysis of toxicity and immune response to the vaccine and of IL-10 -1082 promoter genotype as predictor of disease progression. J Transl Med 6:6. doi:10.1186/1479-5876-6-6
29. Rosenthal JA, Chen L, Baker JL, Putnam D, DeLisa MP (2014) Pathogen-like particles: biomimetic vaccine carriers engineered at the nanoscale. Curr Opin Biotechnol 28:51–58
30. Hollender P, Ittelett D, Villard F, Eymard JC, Jeannesson P, Bernard J (2002) Active matrix metalloprotease-9 in and migration pattern of dendritic cells matured in clinical grade culture conditions. Immunobiology 206(4):441–458
31. Kalchenko V, Shivtiel S, Malina V, Lapid K, Haramati S, Lapidot T, Brill A, Harmelin A (2006) Use of lipophilic near-infrared dye in whole-body optical imaging of hematopoietic cell homing. J Biomed Opt 11(5):050507. doi:10.1117/1.2364903
32. Van den Broeck W, Derore A, Simoens P (2006) Anatomy and nomenclature of murine lymph nodes: descriptive study and nomenclatory standardization in BALB/cAnNCrl mice. J Immunol Methods 312(1–2):12–19
33. Hegde S, Pahne J, Smola-Hess S (2004) Novel immunosuppressive properties of interleukin-6 in dendritic cells: inhibition of NF-kappaB binding activity and CCR7 expression. FASEB J 18(12):1439–1441
34. Kalinski P (2012) Regulation of immune responses by prostaglandin E2. J Immunol 188(1):21–28
35. Delamarre L, Pack M, Chang H, Mellman I, Trombetta ES (2005) Differential lysosomal proteolysis in antigen-presenting cells determines antigen fate. Science 307(5715):1630–1634
36. Savina A, Amigorena S (2007) Phagocytosis and antigen presentation in dendritic cells. Immunol Rev 219:143–156
37. Landi A, Babiuk LA, van Drunen Littel-van den Hurk S (2011) Dendritic cells matured by a prostaglandin E2-containing cocktail can produce high levels of IL-12p70 and are more mature and Th1-biased than dendritic cells treated with TNF-alpha or LPS. Immunobiology 216(6):649–662
38. Dohnal AM, Witt V, Hugel H, Holter W, Gadner H, Felzmann T (2007) Phase I study of tumor Ag-loaded IL-12 secreting semimature DC for the treatment of pediatric cancer. Cytotherapy 9(8):755–770
39. Mailliard RB, Wankowicz-Kalinska A, Cai Q, Wesa A, Hilkens CM, Kapsenberg ML, Kirkwood JM, Storkus WJ, Kalinski P (2004) alpha-type-1 polarized dendritic cells: a novel immunization tool with optimized CTL-inducing activity. Cancer Res 64(17):5934–5937
40. Zobywalski A, Javorovic M, Frankenberger B, Pohla H, Kremmer E, Bigalke I, Schendel DJ (2007) Generation of clinical grade dendritic cells with capacity to produce biologically active IL-12p70. J Transl Med 5:18. doi:10.1186/1479-5876-5-18
41. Spranger S, Javorovic M, Burdek M, Wilde S, Mosetter B, Tippmer S, Bigalke I, Geiger C, Schendel DJ, Frankenberger B (2010) Generation of Th1-polarizing dendritic cells using the TLR7/8 agonist CL075. J Immunol 185(1):738–747
42. Boullart AC, Aarntzen EH, Verdijk P, Jacobs JF, Schuurhuis DH, Benitez-Ribas D, Schreibelt G, van de Rakt MW, Scharenborg NM, de Boer A, Kramer M, Figdor CG, Punt CJ, Adema GJ, de Vries IJ (2008) Maturation of monocyte-derived dendritic cells with Toll-like receptor 3 and 7/8 ligands combined with prostaglandin E2 results in high interleukin-12 production and cell migration. Cancer Immunol Immunother 57(11):1589–1597
43. Marongiu L, Donini M, Toffali L, Zenaro E, Dusi S (2013) ESAT-6 and HspX improve the effectiveness of BCG to induce human dendritic cells-dependent Th1 and NK cells activation. PLoS One 8(10):e75684. doi:10.1371/journal.pone.0075684
44. Spel L, Boelens JJ, Nierkens S, Boes M (2013) Antitumor immune responses mediated by dendritic cells: how signals derived from dying cancer cells drive antigen cross-presentation. Oncoimmunology 2(11):e26403. doi:10.4161/onci.26403
45. Christian NA, Benencia F, Milone MC, Li G, Frail PR, Therien MJ, Coukos G, Hammer DA (2009) In vivo dendritic cell tracking using fluorescence lifetime imaging and near-infrared-emissive polymersomes. Mol Imag Biol 11(3):167–177
46. Park CG, Takahara K, Umemoto E, Yashima Y, Matsubara K, Matsuda Y, Clausen BE, Inaba K, Steinman RM (2001) Five mouse homologues of the human dendritic cell C-type lectin, DC-SIGN. Int Immunol 13(10):1283–1290
47. Robson NC, Hoves S, Maraskovsky E, Schnurr M (2010) Presentation of tumour antigens by dendritic cells and challenges faced. Curr Opin Immunol 22(1):137–144
48. Soudja SM, Henri S, Mello M, Chasson L, Mas A, Wehbe M, Auphan-Anezin N, Leserman L, Van den Eynde B, Schmitt-Verhulst AM (2011) Disrupted lymph node and splenic stroma in mice with induced inflammatory melanomas is associated with impaired recruitment of T and dendritic cells. PLoS One 6(7):e22639. doi:10.1371/journal.pone.0022639
49. Inoue M, Senju S, Hirata S, Irie A, Baba H, Nishimura Y (2009) An in vivo model of priming of antigen-specific human CTL by Mo-DC in NOD/Shi-scid IL2rgamma(null) (NOG) mice. Immunol Lett 126(1–2):67–72
50. Spranger S, Frankenberger B, Schendel DJ (2012) NOD/scid IL-2Rg(null) mice: a preclinical model system to evaluate human dendritic cell-based vaccine strategies in vivo. J Transl Med 10:30. doi:10.1186/1479-5876-10-30
51. Dubensky TW Jr, Reed SG (2010) Adjuvants for cancer vaccines. Semin Immunol 22(3):155–161. doi:10.1016/j.smim.2010.04.007
52. O'Neill DW, Adams S, Bhardwaj N (2004) Manipulating dendritic cell biology for the active immunotherapy of cancer. Blood 104(8):2235–2246
53. Hansen M, Met O, Svane IM, Andersen MH (2012) Cellular based cancer vaccines: type 1 polarization of dendritic cells. Curr Med Chem 19(25):4239–4246